American Journal of Mechanical and Materials Engineering
2025, Vol. 9, No. 1, pp. 25-36
https://doi.org/10.11648/j.ajmme.20250901.13

Research Article

Advanced Modeling and Optimization of Weldment Responses Using Statistical and Metaheuristic Techniques

Aiyemo Williams Otimeyin*, Joseph Ifeanyi Achebo, Uwoghiren Frank

Department of Production Engineering, University of Benin, Benin City, Nigeria

Abstract

Welding process optimization plays a crucial role in enhancing the material properties of weldments and ensuring high-quality outcomes in industrial applications. This study focuses on developing a robust framework for optimizing welding parameters to improve weldment properties, specifically carbon content. Understanding the effects of welding parameters — current, voltage, and gas flow rate — on carbon content is essential for reducing defects, improving weld quality, and achieving cost efficiency. The experiment was conducted at the Petroleum Training Institute (PTI), Warri, utilizing a Central Composite Design (CCD) to systematically analyze the interactions and effects of the welding parameters. A total of 20 experimental runs, including factorial points, axial points, and central replicates, were performed to ensure comprehensive evaluation and error estimation. Response Surface Methodology (RSM) was employed to develop predictive models, while Particle Swarm Optimization (PSO) was applied to refine the optimization process, leveraging its ability to identify global optima in complex solution spaces. The results demonstrate the effectiveness of combining RSM and PSO for advanced welding process optimization. RSM achieved a minimized predicted carbon content of 0.080 mole, with an experimental validation of 0.0518 mole. PSO further enhanced the optimization, predicting a carbon content of 0.0237 mole and achieving an experimental value of 0.0309 mole, demonstrating superior performance in minimizing carbon content. These findings underscore the potential of integrating statistical modeling with metaheuristic techniques to achieve precise control over welding parameters and deliver actionable insights for industrial applications.

Keywords

ANOVA, RSM, PSO, CCD, Desirability, Carbon Content

1. Introduction

Welding is a fundamental process in manufacturing industries, serving as the backbone for constructing durable and functional joints in a wide variety of materials and structures. Its applications range from small-scale fabrications to large industrial infrastructures, highlighting its indispensability across sectors such as automotive, aerospace, construction, and oil and gas. However, despite its extensive use, achieving consistent and high-quality welds remains a significant challenge. This is primarily due to the complex interplay of multiple process parameters, such as current, voltage, gas flow rate, and their influence on the physical and mechanical properties of weldments [1] and [2]. Traditional approaches to welding often rely on manual adjustments and operator expertise, leading to variability in outcomes, inefficiencies, and

*Corresponding author: saywilliams12@gmail.com (Aiyemo Williams Otimeyin)

Received: 29 January 2025; **Accepted:** 14 February 2025; **Published:** 26 February 2025

increased production costs [3] and [4]. These limitations emphasize the urgent need for systematic, science-based methods to optimize welding processes.

In recent years, advancements in computational and statistical methodologies have transformed the way welding processes are studied and optimized. Among these approaches, Response Surface Methodology (RSM) has emerged as a robust statistical tool for developing predictive models that elucidate the relationships between process parameters and weldment properties [5] and [6]. RSM enables researchers to systematically analyze parameter interactions, including linear, quadratic, and interaction effects, to better understand their combined influence on weld quality. For example, parameters like current, voltage, and gas flow rate can significantly impact critical properties such as carbon content, hardness, and structural integrity [7] and [8]. By providing a structured approach to modeling and experimentation, RSM supports data-driven decision-making, reduces the need for extensive trial-and-error testing, and enhances the reliability of predictions [9] and [10].

While RSM provides a strong foundation for process modeling, it is often complemented by optimization techniques to identify the best parameter settings. Metaheuristic algorithms like Particle Swarm Optimization (PSO) have gained attention for their ability to efficiently navigate complex and multifactorial solution spaces [11] and [12]. Inspired by the collective intelligence of natural swarms, PSO is particularly well-suited for welding process optimization, where the search for global optima involves balancing multiple objectives and constraints [13] and [14]. By integrating the predictive modeling capabilities of RSM with the optimization power of PSO, this study aims to establish a comprehensive framework for welding process optimization. The synergistic use of these methods allows for precise control over welding parameters, minimizes defects, and enhances the overall quality and efficiency of welds [15] and [16].

This research not only seeks to advance theoretical understanding but also strives to provide practical guidelines for industrial applications [17] and [18]. By addressing the challenges associated with parameter variability and process inefficiencies, the findings contribute to bridging the gap between research and practice [19] and [20]. Ultimately, this study aims to facilitate the adoption of more scientifically grounded and efficient welding practices, enabling manufacturers to achieve superior results while reducing operational costs and material waste [21] and [22]. The integration of advanced computational models and optimization algorithms highlights the evolving nature of welding research and its alignment with modern manufacturing demands [23] and [24].

Furthermore, this study builds upon previous investigations into welding processes, leveraging insights from diverse applications such as aerospace, automotive, and heavy engineering industries [25] and [26]. The inclusion of modern methodologies, such as Six Sigma and finite element modeling, has also contributed to the enhancement of weld quality and reliability [27] and [28]. By drawing on these advancements, the present research provides a comprehensive framework for tackling welding challenges across varied contexts [29] and [30].

The practical implications of this research are significant. For instance, in high-demand sectors like shipbuilding and energy, where weld quality is critical, the use of advanced techniques can lead to substantial improvements in productivity and safety [31] and [32]. Moreover, the growing adoption of hybrid welding technologies has further expanded the scope of process optimization, allowing for the integration of laser and arc welding methods [33] and [34]. These developments underline the importance of continuous innovation and knowledge-sharing in the field of welding science [35] and [36].

In conclusion, by leveraging advancements in statistical modeling and optimization, this study provides a roadmap for enhancing welding practices, improving weld quality, and reducing production costs. The insights gained are expected to benefit both researchers and practitioners, contributing to the broader goal of achieving excellence in welding technology [37].

2. Materials and Methods

2.1. Experimental Design

The experiment was conducted at the Petroleum Training Institute (PTI), Warri. Central Composite Design (CCD) was utilized to systematically study the influence of three key welding parameters: Current (A) 159.77 to 210.23, Voltage (V) 18.98 to 24.02, and Gas Flow Rate (L/min) 10.98 to 16.02. CCD is a robust experimental design methodology that allows for the evaluation of linear, quadratic, and interaction effects of factors on a given response. The experimental matrix consisted of 20 runs, including factorial points, axial points, and central replicates to estimate pure error. The response variable investigated in this study was the carbon content of weldments, measured in moles. Table 1 provides the experimental conditions and observed results.

Table 1. *Experimental results.*

Run	A: Current (A)	B: Voltage (V)	C: Gas Flow Rate (L/min)	Response: Carbon Content (mole)
1	170	20	12	0.1802
2	185	21.5	13.5	0.161
3	200	23	15	0.121
4	159.773	21.5	13.5	0.122
5	170	20	15	0.181
6	170	23	12	0.156
7	185	21.5	10.9773	0.102
8	185	21.5	13.5	0.165
9	185	24.0227	13.5	0.199
10	210.227	21.5	13.5	0.17
11	185	21.5	13.5	0.163
12	200	23	12	0.176
13	185	21.5	16.0227	0.087
14	185	21.5	13.5	0.216
15	200	20	15	0.196
16	200	20	12	0.179
17	185	21.5	13.5	0.163
18	185	21.5	13.5	0.161
19	170	23	15	0.113
20	185	18.9773	13.5	0.252

2.2. Statistical Modeling

The experimental data were analyzed using Response Surface Methodology (RSM) to develop predictive models for carbon content. A second-order polynomial regression model was adopted due to its flexibility in capturing curvature and interactions among factors. The general form of the model is expressed as:

$$y_i = f(x_i, \beta) + e_i \tag{1}$$

where y_i represents the response (carbon content), x_i are the independent variables (welding parameters), coefficients (β) are determined through regression analysis, and represents random error (e_i).

The adequacy of the model was assessed using Analysis of Variance (ANOVA), which evaluated the significance of individual terms and the overall model fit. To ensure accuracy and reliability, diagnostics such as predicted vs. actual plots, contour plots, surface plots, and R-squared values were examined. These visual and statistical analyses provided insights into the model's performance and highlighted the interactions between parameters.

2.3. Optimization Using PSO

Particle Swarm Optimization (PSO) was employed to determine the optimal combination of welding parameters that maximize carbon content while minimizing weld defects. PSO is a bio-inspired optimization algorithm based on the collective behavior of swarms in nature. The algorithm initializes a population of particles, each representing a potential solution. These particles navigate the solution space by updating their positions based on individual and collective experiences, guided by objective function evaluations.

In this study, the objective function incorporated the predictive model derived from RSM, enabling PSO to efficiently explore the parameter space. Key algorithmic parameters, including swarm size, cognitive and social coefficients, and maximum iterations, were fine-tuned to balance exploration and exploitation.

2.4. Validation

The validity of the RSM model and PSO-optimized solutions was verified through experimental trials conducted under the predicted optimal conditions. The results of these trials were compared with the model predictions to assess the accuracy of the approach. Additionally, the robustness of the optimization strategy was tested by slightly varying the input parameters to observe the consistency of the outcomes.

2.5. Measurement of Carbon Content

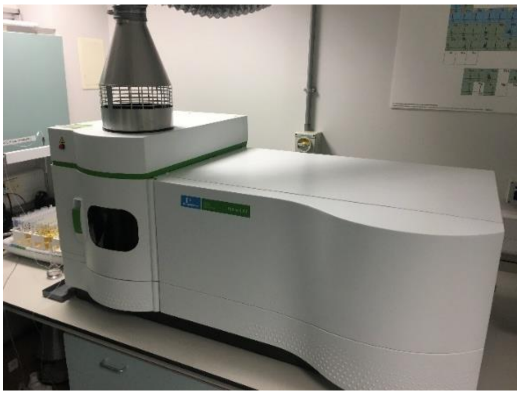

Figure 1. Optical Emission Spectrometry.

The carbon content in the weldments was measured using Optical Emission Spectrometry (OES), a highly precise and rapid technique for analyzing metal compositions. The OES system vaporizes a small portion of the sample and analyzes the emitted light spectrum to determine elemental concentrations. This method was chosen for its accuracy, speed, and suitability for metallurgical applications.

3. Results and Discussion

3.1. Statistical Modeling and ANOVA Analysis

The results of the Analysis of Variance (ANOVA) in Table 2 for the quadratic model revealed that the model was statistically significant, with a p-value of 0.0009 and an F-value of 9.24. Among the individual factors, voltage (B) and gas flow rate (C) exhibited significant effects on carbon content, as indicated by their respective p-values of 0.0010 and 0.0450. These findings highlight the critical influence of voltage and gas flow rate in determining weldment properties.

The interaction effects between current and voltage (AB) and current and gas flow rate (AC) were not statistically significant, with p-values of 0.7843 and 0.9354, respectively. However, the interaction between voltage and gas flow rate (BC) showed a significant impact, with a p-value of 0.0448. This underscores the importance of considering parameter interactions when optimizing welding processes. The lack of fit was not significant (p = 0.8722), indicating that the model provided an adequate representation of the data.

Table 2. ANOVA for Quadratic model for Carbon.

Source	Sum of Squares	df	Mean Square	F-value	p-value	
Model	0.0265	9	0.0029	9.24	0.0009	significant
A-Current	0.0007	1	0.0007	2.34	0.1573	
B-Voltage	0.0067	1	0.0067	21.03	0.001	
C-Gas Flow Rate	0.0017	1	0.0017	5.24	0.045	
AB	0	1	0	0.0791	0.7843	
AC	2.21E-06	1	2.21E-06	0.0069	0.9354	
BC	0.0017	1	0.0017	5.26	0.0448	
A^2	0.0008	1	0.0008	2.37	0.1548	
B^2	0.0063	1	0.0063	19.69	0.0013	
C^2	0.0093	1	0.0093	29.27	0.0003	
Residual	0.0032	10	0.0003			
Lack of Fit	0.0008	5	0.0002	0.3353	0.8722	not significant
Pure Error	0.0024	5	0.0005			
Cor Total	0.0297	19				

The fit statistics of Table 3, including an R-squared value of 0.8927 and an adjusted R-squared value of 0.7961, confirm the reliability and accuracy of the model. The adequate precision value of 13.9335 further supports the model's capability to navigate the design space effectively.

Table 3. *Fit Statistics Carbon.*

Std. Dev.	0.0179	R^2	0.8927
Mean	0.1632	Adjusted R^2	0.7961
C.V. %	10.94	Predicted R^2	0.6748
		Adeq Precision	13.9335

3.2. Predictive Modeling and Visualization

The predictive model for carbon content is expressed in Equation (2), while Figure 2 depicts the predicted versus actual plot. The contour plot and surface plot for carbon content are presented in Figures 3 and 4, respectively.

The predicted versus actual plot in Figure 2 demonstrates a strong correlation, highlighting the model's effectiveness in accurately capturing trends within the experimental data. Additionally, the contour and surface plots provide valuable visual insights into the interactions between parameters and their influence on carbon content. These visualizations reveal optimal regions for parameter settings, aiding in the identification of conditions that minimize carbon content.

$$Carbon = 0.032273 + 0.010490A - 0.339233B + 0.434207C + 0.000079AB + 0.000023AC - 0.006433BC - 0.000032A^2 + 0.009275B^2 - 0.011309C^2 \quad (2)$$

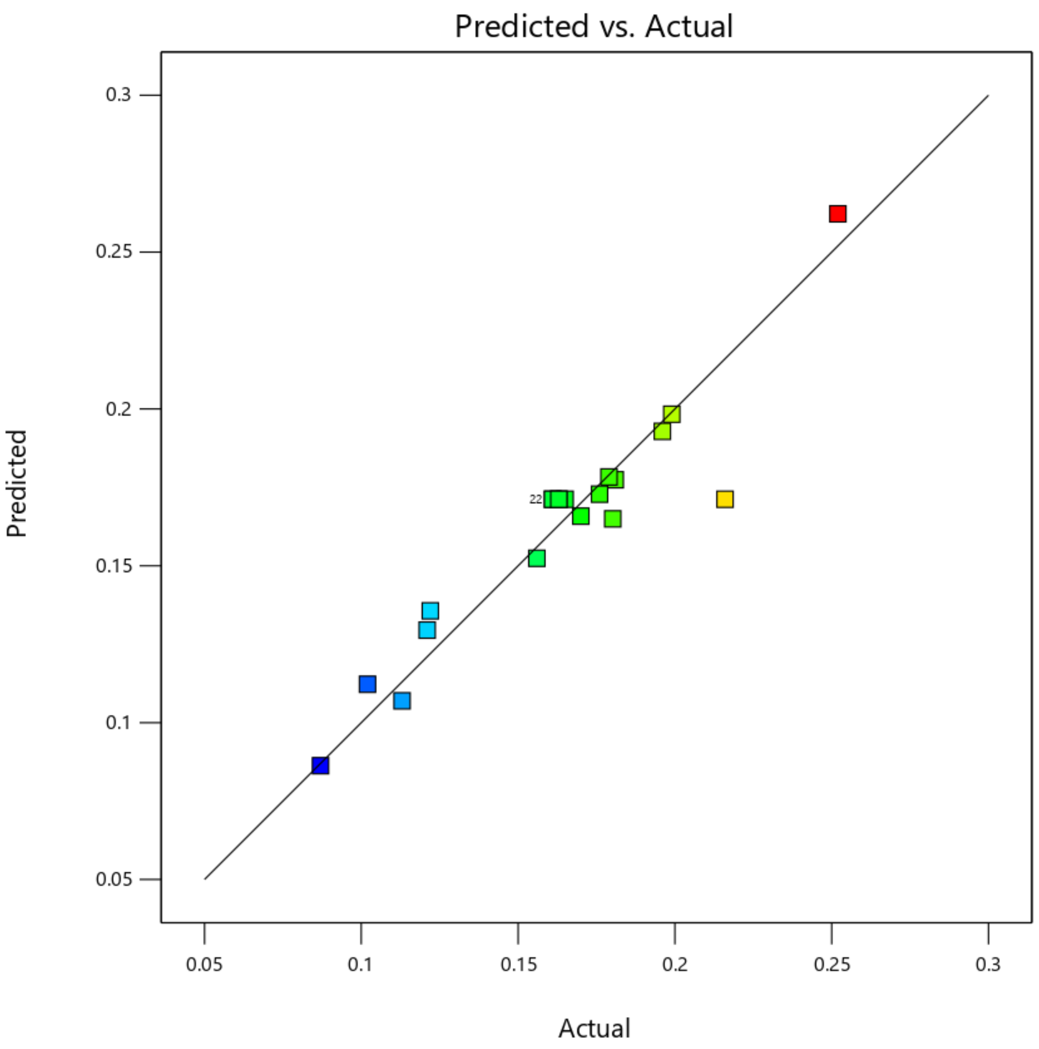

Figure 2. *Predicted versus actual plot for carbon content.*

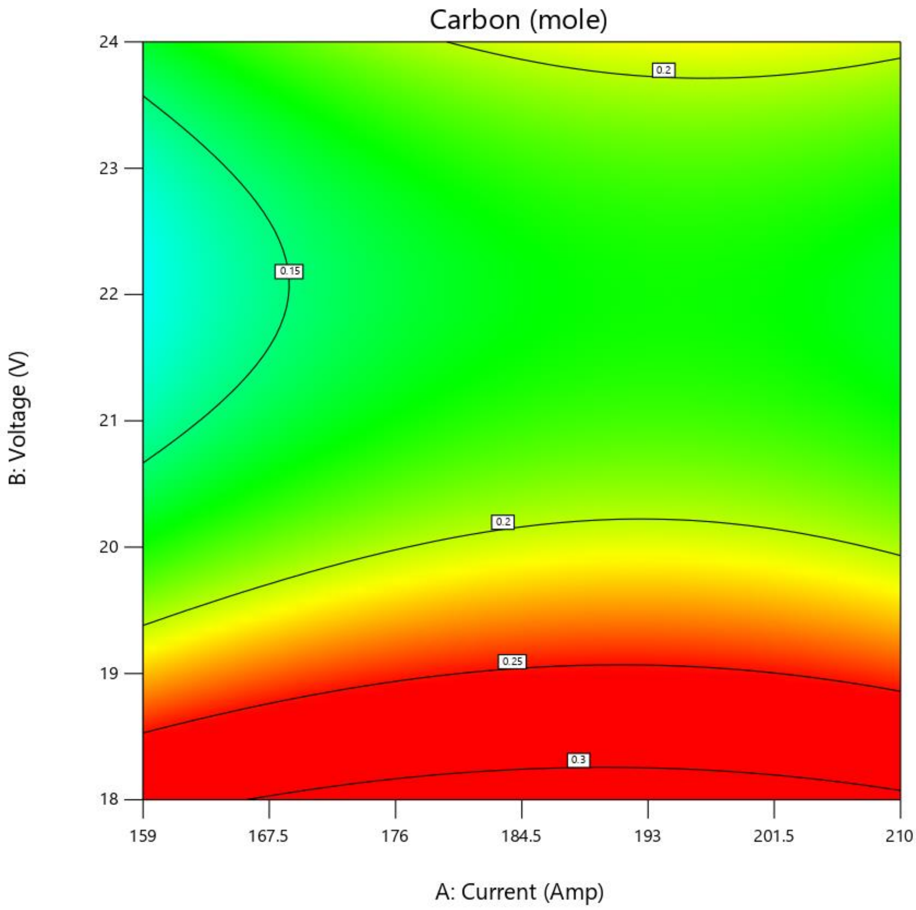

Figure 3. Contour plot for Carbon Content.

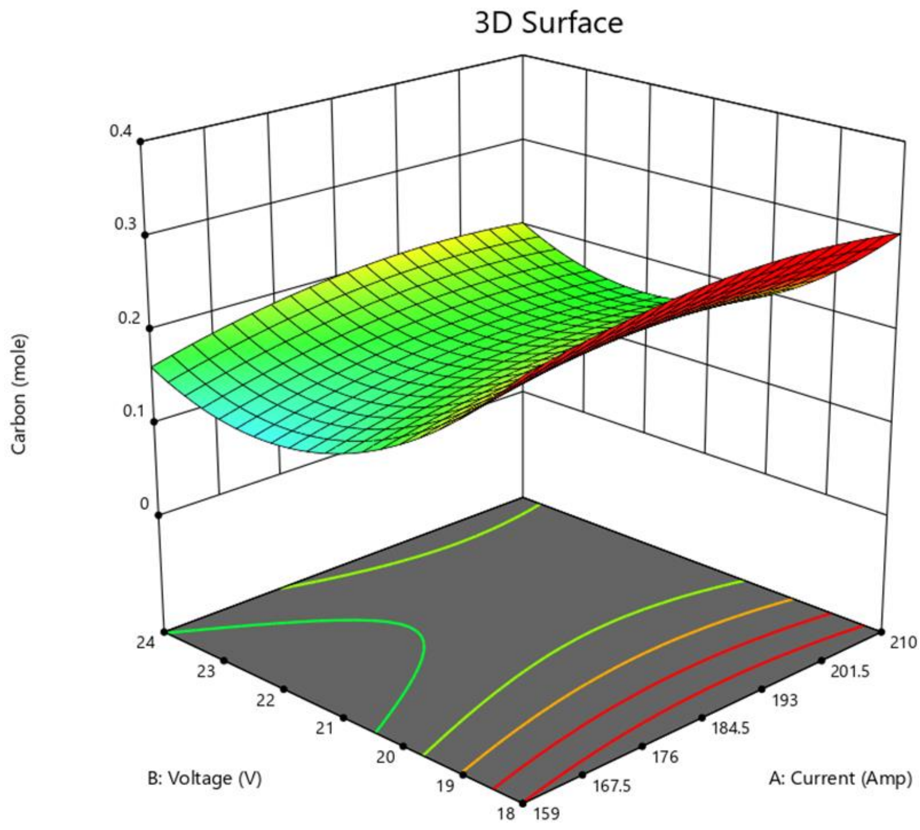

Figure 4. Contour plot for Carbon Content.

3.3. Optimization Results

3.3.1. Response Surface Methodology (RSM)-based Optimization

The constraints for optimization are presented in Table 4. Using Response Surface Methodology (RSM)-based optimization, the optimal parameter settings were identified as Current = 159 A, Voltage = 22.907 V, and Gas Flow Rate = 15.072 L/min (as shown in Table 5). These conditions yielded a predicted carbon content of 0.080 mole. Experimental validation under these optimized conditions resulted in a carbon content of 0.0518 mole, demonstrating strong agreement with the predicted value and confirming the model's accuracy.

Table 4. Constraints for optimization using Design Expert 13.

Name	Goal	Lower Limit	Upper Limit	Lower Weight	Upper Weight	Importance
A:Current	is in range	159	210	1	1	3
B:Voltage	is in range	18	24	1	1	3
C:Gas Flow Rate	is in range	10	16	1	1	3
Carbon	minimize	0.087	0.252	1	1	3
Sulphur	minimize	0.019	0.033	1	1	3
Hydrogen	minimize	5.11	6.64	1	1	3
Cracking ratio	minimize	23.33	49.2	1	1	3
Hardness Number	maximize	125.79	137.11	1	1	3

Table 5. Optimization solutions using Response Surface Methodology (RSM).

Number	Current	Voltage	Gas Flow Rate	Carbon	Desirability	
1	159	22.907	15.072	0.08	0.931	Selected
2	159	22.93	15.078	0.08	0.931	
3	159	22.94	15.081	0.08	0.931	
4	159	22.989	15.087	0.08	0.931	

3.3.2. Particle Swarm Optimization (PSO)

The Particle Swarm Optimization (PSO) process is visualized through the Performance Plot, Particle Trajectories, Evolution of the Best Solution Component, and Fitness Landscape Plot, shown in Figures 5, 6, 7, and 8, respectively. These plots illustrate the refined optimization process, which achieved a minimized carbon content of 0.0237 mole at the optimized parameter settings of Current = 159.77 A, Voltage = 23.1637 V, and Gas Flow Rate = 16.02 L/min.

Table 6. PSO Optimization solutions for Carbon.

s/n	Current	Voltage	Gas Flow Rate	Carbon
1	159.77	23.1637	16.02	0.023715
2	159.77	23.1637	16.02	0.023715

s/n	Current	Voltage	Gas Flow Rate	Carbon
3	159.77	23.1637	16.02	0.023715
4	159.77	23.16367	16.02	0.023715

The PSO algorithm outperformed the RSM approach in minimizing carbon content, as demonstrated in Table 7. Experimental validation under these optimized conditions yielded a carbon content of 0.0309 mole, confirming the model's accuracy and the efficacy of the PSO algorithm.

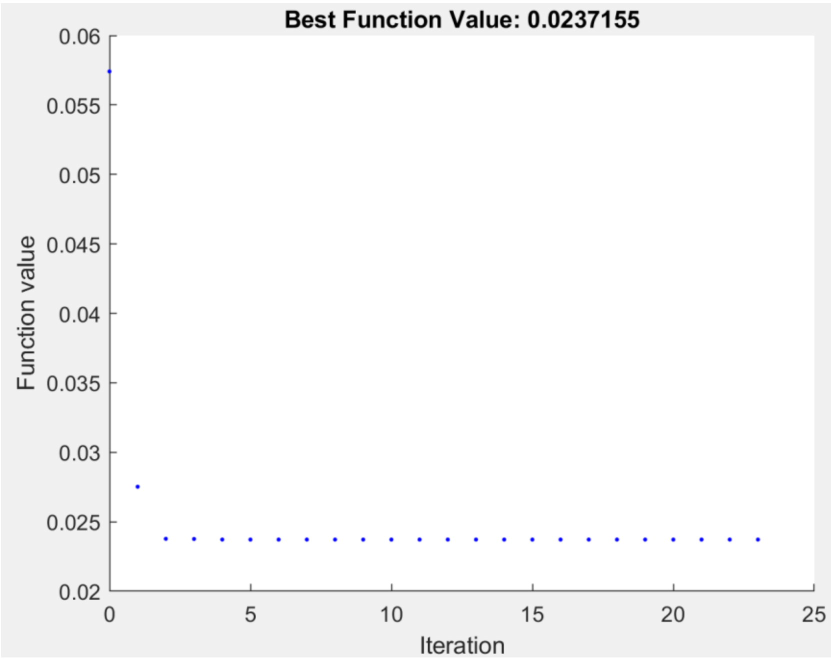

***Figure 5**. PSO Performance Plot for Carbon Content.*

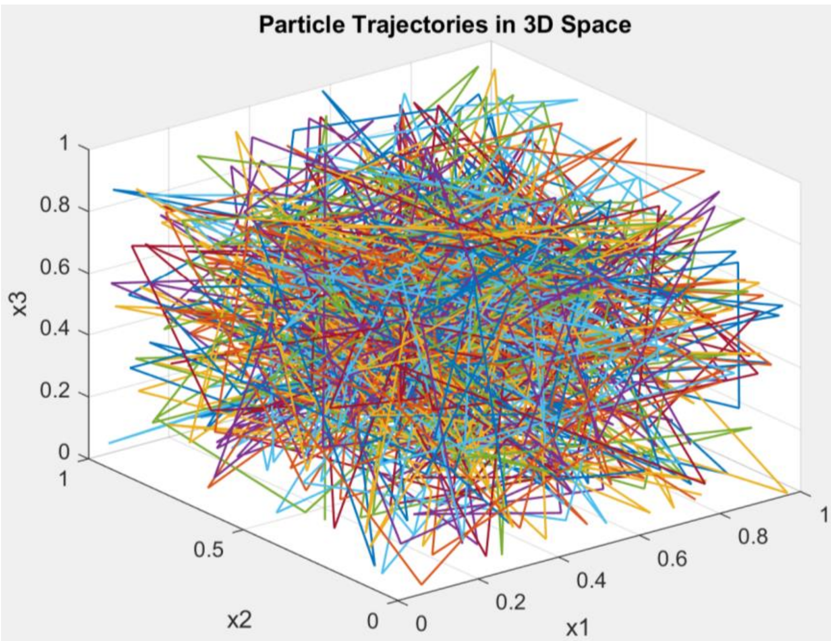

***Figure 6**. Plot of PSO Particle Trajectories in 3d space for Carbon Content.*

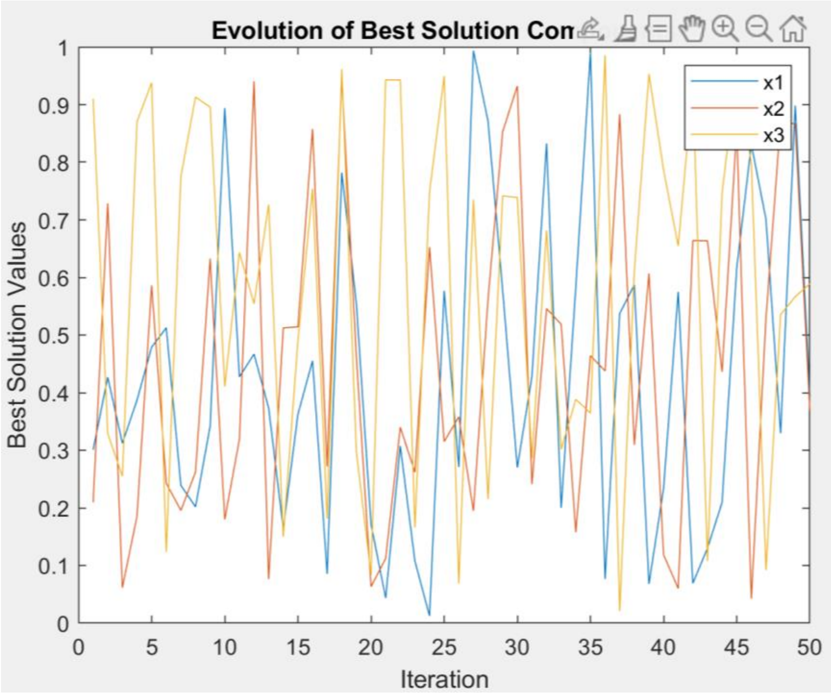

Figure 7. Plot of PSO Evolution of Best Solution Component for Carbon Content.

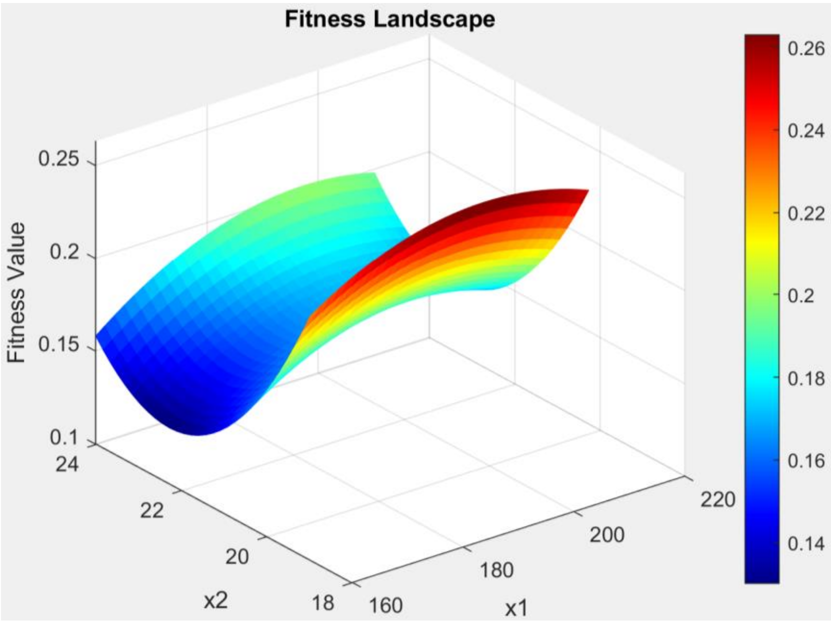

Figure 8. PSO Plot of Fitness Landscape for Carbon Content.

3.3.3. Comparative Analysis of RSM and PSO

Table 7 provides a comparative analysis of the experimental, RSM, and PSO results, highlighting the superior performance of the PSO algorithm in achieving lower carbon content values. The fitness landscape and particle trajectories, illustrated in Figures 5 through 8, further demonstrate PSO's efficacy in exploring the solution space and identifying global optima.

While RSM predicted a carbon content of 0.08 mole and achieved an experimental value of 0.0518 mole, the PSO algorithm achieved a lower experimental carbon content of 0.0309 mole, closely aligning with its predicted value of 0.0237 mole. This demonstrates PSO's ability to refine the optimization process and minimize errors effectively.

Table 7. *Optimization Comparison between Experimental Value, RSM and PSO algorithm.*

	Actual	Predicted	Error
RSM	0.0518	0.08	-0.0282
PSO	0.0309	0.023715	0.007185

3.4. Practical Implications and Guidelines

The findings of this study provide actionable insights for optimizing welding processes in industrial applications. By integrating Response Surface Methodology (RSM) and Particle Swarm Optimization (PSO), practitioners can achieve precise control over welding parameters, minimize defects, and enhance weld quality. This combination offers a reliable approach for improving process efficiency and achieving superior results.

One key takeaway from the study is the importance of understanding parameter interactions and their collective effects on weldment properties. A comprehensive grasp of these relationships allows for more informed and strategic process adjustments, leading to better outcomes in terms of weld strength, durability, and overall quality.

The proposed optimization framework offers practical benefits to the industry. It enhances welding efficiency by minimizing trial-and-error experimentation, thereby saving time and resources. Additionally, it helps reduce operational costs by lowering material waste and optimizing energy consumption. Furthermore, the framework ensures consistent outcomes by improving repeatability and reliability in weld quality across diverse operational conditions.

These guidelines serve as a strategic foundation for welding process optimization, making them adaptable to various industrial scenarios. By applying these principles, manufacturers can achieve superior performance, cost-effectiveness, and sustainable practices in their operations.

4. Conclusion

This study highlights the potential of combining Response Surface Methodology (RSM) and Particle Swarm Optimization (PSO) for advanced welding process optimization. The results demonstrate that while RSM achieved a minimized experimental carbon content of 0.0518 mole, PSO further refined the optimization process, achieving an experimental carbon content of 0.0309 mole, closely aligning with its predicted value of 0.0237 mole. These findings underscore the superior performance of PSO in navigating the solution space and identifying global optima.

By integrating robust statistical modeling with metaheuristic techniques, this research offers actionable insights and practical tools for enhancing weld quality. The study also emphasizes the importance of understanding parameter interactions and their effects on weldment properties, providing a foundation for achieving precise control over process variables, reducing defects, and improving efficiency.

Future work could explore extending this methodology to optimize other material properties, welding techniques, and process conditions. This approach has the potential to further advance industrial applications by offering more efficient, cost-effective, and sustainable solutions for complex welding challenges.

Conflicts of Interest

The authors declare no conflicts of interest.

References

[1] Abhishek, P., Raj, K. B., and Siva, S. R. (2016): Parametric Optimization of Tungsten Inert Gas (TIG) Welding by using Taguchi Approach. International Journal of Innovative Research in Science, Engineering and Technology, Vol. 5, Issue 3.

[2] Achebo, J. and Odinikuku, W. E. (2015): Optimization of Gas Metal Arc Welding Process Parameters Using Standard Deviation (SDV) and Multi-Objective Optimization on the Basis of Ratio Analysis (MOORA). Journal of Minerals and Materials Characterization and Engineering (JMMCE), 3, pp. 298-308.

[3] Anowa, H. D., Achebo, J. I., Ozigagun, A., and Etin-Osa, E. C. (2018): Analysis of weld molten metal kinematic viscosity of TIG mild steel weld. International Journal of Advanced Engineering and Management Research, 3, ISSN: 2456-3676.

[4] Aoki, Y., Kuroiwa, R., Fujii, H., Murayama, G., and Yasuyama, M. (2019): Linear friction stir welding of medium carbon steel at low temperature. ISIJ International, 59(10), pp. 1853–1859. https://doi.org/10.2355/isijinternational.ISIJINT-2018-458

[5] Bhadeshia, H. K. D. H. (2017): The influence of bainite and martensite–austenite constituents on mechanical properties. Materials Science and Technology, 33, pp. 1869–1874. https://doi.org/10.1080/02670836.2017.1371971

[6] Choi, J. W., Li, W., Ushioda, K., Yamamoto, M., and Fujii, H. (2022): Strengthening mechanism of high-pressure linear friction welded AA7075-T6 joint. Materials Characterization, 191, p. 112112. https://doi.org/10.1016/j.matchar.2022.112112

[7] Choudhury, B., and Chandrasekaran, M. (2017): Investigation on welding characteristics of aerospace materials – A review. Materials Today: Proceedings, 4, pp. 7519–7526. https://doi.org/10.1016/j.matpr.2017.07.083

[8] Deutsches Institut DIN, für Normung e. V. (2023): Schweißen - Schmelzschweißverbindungen an Stahl, Nickel, Titan und deren Legierungen (ohne Strahlschweißen) - Bewertungsgruppen von Unregelmäßigkeiten (ISO 5817: 2023). Berlin: DIN Media GmbH.

[9] Erhunmwun, I. D. and Etin-Osa, C. E. (2019): Temperature distribution in centrifugal casting with partial solidification during pouring. Materials and Engineering Technology, ISSN: 2667-4033.

[10] Etin-Osa, C. E. and Achebo, J. I. (2017): Analysis of optimum butt welded joint for mild steel components using FEM (ANSYS). American Journal of Naval Architecture and Marine Engineering, 2(3), pp. 61-70.

[11] Etin-Osa, E. C. and Ogbeide, O. O. (2021): Optimization of the weld bead volume of tungsten inert gas mild steel using response surface methodology. NIPES Journal of Science and Technology Research, 3(4), pp. 314-321.

[12] Haslberger, P., Holly, S., Ernst, W., and Schnitzer, R. (2018): Microstructure and mechanical properties of high-strength steel welding consumables with a minimum yield strength of 1100 MPa. Journal of Materials Science, 53, pp. 6968–6979. https://doi.org/10.1007/s10853-018-2042-9

[13] Hobbacher, A. & Kassner, M. (2012): On relation between fatigue properties of welded joints, quality criteria and groups in ISO 5817. Welding World, 56(11–12), pp. 153–169. https://doi.org/10.1007/BF03321405

[14] Imhansoloeva, N. A., Achebo, J. I., Obahiagbon, K., Osarenmwinda, J. O., and Etin-Osa, C. E. (2018): Optimization of the deposition rate of tungsten inert gas mild steel using response surface methodology. Scientific Research Publishing, 0, pp. 784-804.

[15] Jamrozik, W., Górka, J., and Kik, T. (2021): Temperature-based prediction of joint hardness in TIG welding of Inconel 600, 625, and 718 nickel superalloys. Materials, 14, p. 442. https://doi.org/10.3390/ma14020442

[16] Jorge, J. C. F., Souza, L. F. G. D., Mendes, M. C., Bott, I. S., Araújo, L. S., Santos, V. R. D., Rebello, J. M. A., and Evans, G. M. (2021): Microstructure characterization and its relationship with impact toughness of C-Mn and high-strength low alloy steel weld metals - a review. Journal of Materials Research and Technology, 10, pp. 471–501. https://doi.org/10.1016/j.jmrt.2020.12.006

[17] Kataria, R., Pratap Singh, R., Sharma, P., and Phanden, R. K. (2021): Welding of super alloys: A review. Materials Today: Proceedings, 38, pp. 265–268. https://doi.org/10.1016/j.matpr.2020.07.198

[18] Kuroiwa, R., Liu, H., Aoki, Y., Yoon, S., Fujii, H., Murayama, G., and Yasuyama, M. (2020): Microstructure control of medium carbon steel joints by low-temperature linear friction welding. Science and Technology of Welding and Joining, 25(1), pp. 1–9. https://doi.org/10.2355/isijinternational.ISIJINT-2018-458

[19] Lee, D., Song, H., Lee, J. H., and Babu, S. S. (2016): Influence of grain boundary ferrite on toughness variability in HSLA steels. Materials Characterization, 111, pp. 390–397. https://doi.org/10.1016/j.matchar.2015.10.005

[20] Li, S., Liu, Q., Rui, S.-S., et al. (2022): Fatigue crack initiation behaviors around defects induced by welding thermal cycle in superalloy IN617B. International Journal of Fatigue, 158, p. 106745. https://doi.org/10.1016/j.ijfatigue.2022.106745

[21] Lu, S., Lu, Y., Shen, H., Chen, Y., Zhang, Z., and Sun, X. (2019): Investigation on microstructure and mechanical properties of a low-temperature multi-pass tungsten inert gas welding process. Journal of Materials Processing Technology, 265, pp. 1-9. https://doi.org/10.1016/j.jmatprotec.2018.09.032

[22] Mani, K., Uthayakumar, M., Kumar, M. P., and Sekar, K. (2019): Optimization of friction welding parameters on microstructure and mechanical properties of Al6061 and AISI 304 dissimilar joint. Procedia Manufacturing, 30, pp. 505-512. https://doi.org/10.1016/j.promfg.2019.02.071

[23] Masoumi, A., Niknejad, S. R., and Ghassemi, H. (2018): Weld zone properties of micro-alloyed steel joints in TIG welding process: Experimental and numerical analysis. Journal of Materials Engineering and Performance, 27, pp. 2949–2960. https://doi.org/10.1007/s11665-018-3515-1

[24] Mazumder, J., Schifferer, A., and Choi, J. (1999): Direct materials deposition: Designer microstructure for rapid prototyping and solid freeform fabrication. Materials Research Innovations, 3(3), pp. 118-131. https://doi.org/10.1007/s100190050172

[25] Mishra, R. S. and Ma, Z. Y. (2005): Friction stir welding and processing. Materials Science and Engineering: R: Reports, 50(1-2), pp. 1-78. https://doi.org/10.1016/j.mser.2005.07.001

[26] Mughal, M. P., and Sajjad, M. (2022): Application of Six Sigma DMAIC to improve weld quality in shipbuilding. Shipbuilding Technology and Research, 2(4), pp. 234-240.

[27] Nandan, R., Deb Roy, T., and Bhadeshia, H. K. D. H. (2008): Recent advances in friction-stir welding – Process, weldment structure and properties. Progress in Materials Science, 53(6), pp. 980-1023. https://doi.org/10.1016/j.pmatsci.2008.05.001

[28] Ogbeide, O. O., Afolalu, T. D., and Etin-Osa, C. E. (2021): Investigation into microstructural and mechanical properties of friction stir welded aluminum alloy using optimized welding parameters. Journal of Materials Science Research and Reviews, 8(3), pp. 21-30.

[29] Oliveira, J. P., Zeng, Z., and Miranda, R. M. (2017): High speed steel TIG welds with different heat input. Journal of Materials Processing Technology, 246, pp. 1–9. https://doi.org/10.1016/j.jmatprotec.2017.03.019

[30] Pal, S., and Bhattacharya, B. (2016): Study of weld pool temperature and its optimization for better weld quality: A finite element approach. Indian Welding Journal, 49(2), pp. 61-66.

[31] Prabhu, R. T., Swaminathan, J., and Manohar, P. (2020): Experimental analysis and parametric optimization of weld bead geometry in TIG welding of stainless steel. Advances in Materials Science and Engineering, 2020, Article ID 7539826. https://doi.org/10.1155/2020/7539826

[32] Quintana, E., and Amaya, M. (2022): Advances in the development of hybrid laser arc welding processes: A review. Welding in the World, 66(6), pp. 1365–1380. https://doi.org/10.1007/s40194-022-01358-z

[33] Rai, R., Deb Roy, T., and Bhadeshia, H. K. D. H. (2011): Review: Friction stir welding tools. Science and Technology of Welding and Joining, 16(4), pp. 325-342. https://doi.org/10.1179/1362171811Y.0000000023

[34] Rajkumar, K. and Balasubramanian, V. (2008): Effect of pulsed current welding on mechanical properties of high strength aluminum alloy joints. Materials and Design, 29, pp. 1860–1866. https://doi.org/10.1016/j.matdes.2008.02.001

[35] Ravindran, M., and Janarthanan, B. (2019): Investigations on the effect of preheating and post-weld heat treatment on the mechanical and metallurgical properties of TIG welded joints of Inconel 718. Materials Today: Proceedings, 27, pp. 2440-2444. https://doi.org/10.1016/j.matpr.2019.08.187

[36] Shaikh, S., and Chourasia, D. (2021): Mechanical and micro-structural characterization of dissimilar metal TIG welding between austenitic stainless steel and mild steel. Materials Today: Proceedings, 43(Part 2), pp. 1626–1631. https://doi.org/10.1016/j.matpr.2020.12.665

[37] Ogbeide, O. O. and Etin-Osa, E. C., 2023. Prediction of hardness of mild steel welded joints in a tungsten inert gas welding process using artificial neural network. JASEM, 27(11), pp. 2381-2386.